Quarterly Status Report

Subcontract: XDJ-2-30630-27
Title: "Structure of Silicon-Based Thin Film Solar Cell Materials"
Subcontractor: Colorado School of Mines (CSM)
Principal Investigator: Don L. Williamson
NREL Technical Monitor: Bolko von Roedern
NREL Subcontract Associate: Carolyn Lopez
CSM Subcontract Administrator: Levona DeHerrera
Project period: 03/01/04 - 05/31/04

Summary
During this third quarter of Phase II of the NREL subcontract we have addressed issues related to Tasks 1,2 and 3: Task 1 - Electron Microscopy and Spectrometry Experiments, Task 2 - Small-angle Scattering Experiments, and Task 3 - Wide-angle X-ray Diffraction Experiments. Specific experiments and results from each of the tasks are presented below.

Discussion

Task 1

A proposal for instrument time at Brookhaven National Laboratory (BNL) was written and submitted at the request of Eli Sutter to allow her to continue transmission electron microscopy measurements of relevant samples for our NREL subcontract. She is now in charge of the Electron Microscopy Cluster of instruments at BNL and is interested in continuing to help with the project. A total of 3 days of time was requested in the next cycle (Sept-Dec, 04) to study specifically the issue of Ge clustering in a-SiGe:H alloys. The specific instrument requested was the JEOL3000F 300kV scanning/transmission electron microscope because of its EELS and EDS capabilities. Ge distribution maps on the nanoscale will be a major goal of the measurements.

Tasks 2 and 3

Three films of a-Si:H solar cell material grown on Al foil and stainless steel were supplied by R. Schropp of Utrecht University for SAXS, XRD and density measurements. The film structures are listed in Table 1. All were made by HWCVD. The goal was to confirm a substrate template effect on the microstructure, initial evidence for which was presented in the quarterly report CSM5Q-11-30-2003.

Table 1. Film structures for SAXS (on Al foil) and XRD (on stainless steel-SS). The films with same layer structure on Al and SS were made side-by-side in the same run. [However, the label numbers supplied by Utrecht – written on the boxes/plastic bags holding each sample were not clearly different, so CSM sample numbers were introduced].

Sample No. (CSM)	Label # (Utrecht)	Layer structure
1-Al	P3264	a-Si:H (2 μm-intrinsic)/Al
1-SS	P3286	a-Si:H (2 μm-intrinsic)/SS
2-Al	P3264	a-Si:H (2 μm-intrinsic)/a-Si:H(50 nm-n-layer)/Al
2-SS	P3264	a-Si:H (2 μm-intrinsic)/a-Si:H(50 nm-n-layer)/SS
3-Al	P3286	a-Si:H (2 μm-intrinsic)/μc-Si:H(50 nm-n-layer)/Al
3-SS	P3286	a-Si:H (2 μm-intrinsic)/μc-Si:H(50 nm-n-layer)/SS

First, all the SAXS results and the analyses will be presented. These will be followed by the XRD results and analyses. Then the flotation density data will be presented and analyzed. Finally, summary comments of all the results will be made.

Figure 1 shows the SAXS results from the 3 films. Sample 1-Al and 2-Al show similar SAXS while 3-Al shows a significantly larger signal at low q indicating some larger-scale scattering features. The solid lines through the data are fits based on distributions of spheres. A Porod term [1] was included to fit the 3-Al data. A size distribution for one of the films is shown in the inset. One sample (1-Al) was tilted also measured at 45 degrees relative to the SAXS beam. A slightly reduced SAXS signal upon tilting indicates somewhat elongated scattering features aligned along the growth direction. Quantitative results from the SAXS data analysis are listed in Table 2.

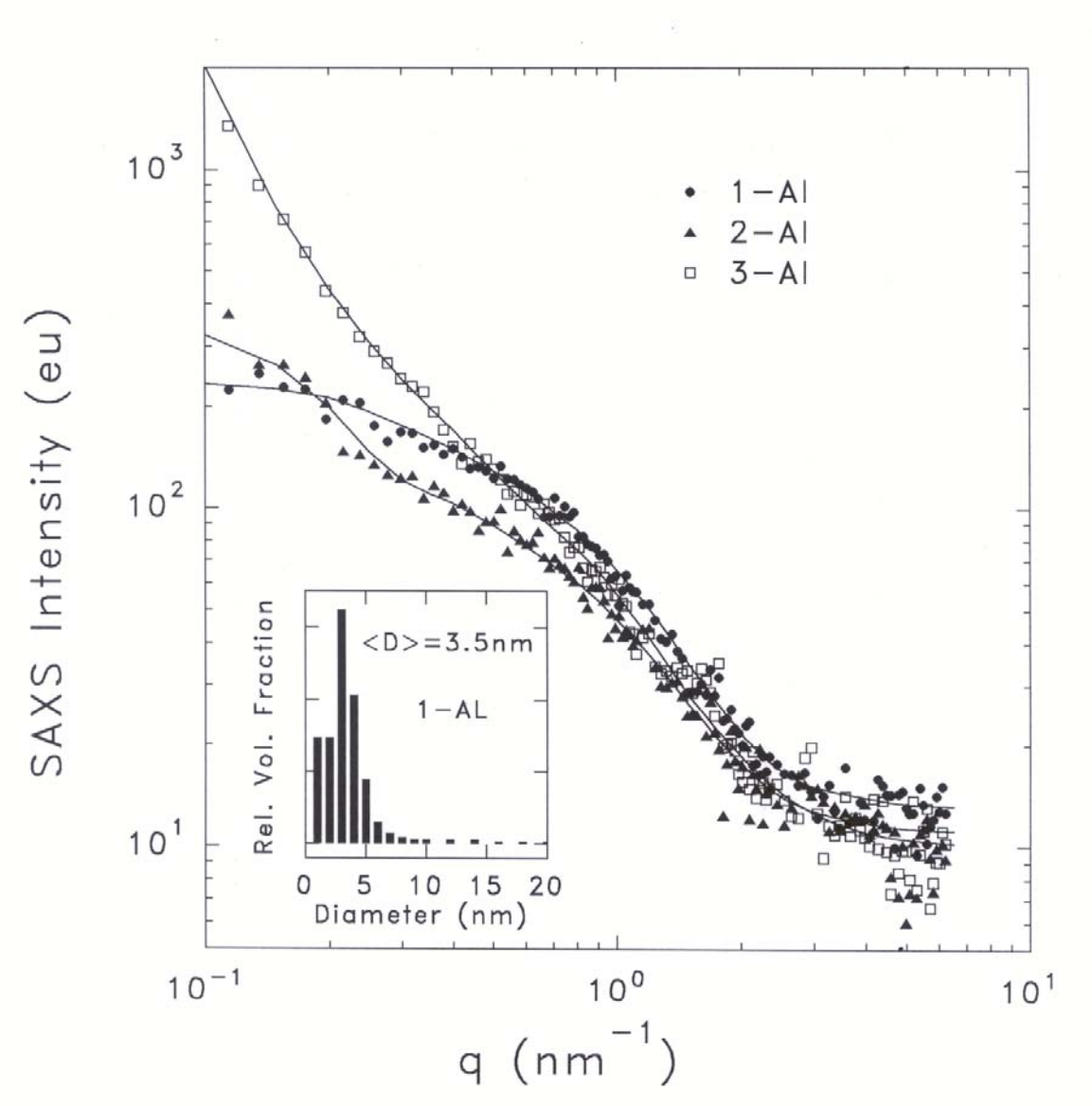

Fig. 1. SAXS data (symbols) and fits (lines) for the three Utrech films on Al foil. Inset shows sphere size distribution for one film.

Table 2. Quantitative SAXS results.

Sample No.	Q_N (10^{23} eu/cm^3)	Q_T (10^{23} eu/cm^3)	I_d (eu)	<D> (nm)	D_{mp} (nm)	f_{max} (vol.%)
1-Al	2.50	2.50	13	3.5	3.0	0.15
2-Al	1.83	1.83	11	3.8	3.0	0.11
3-Al	2.31	2.87	10	3.3	2.0	0.13

Q_N represents the integrated SAXS [1] from the nanostructural features that have sizes fitted by the distribution of spheres. Q_T represent the total integrated SAXS which includes the rising SAXS at the lowest angles that correspond to larger features (> 20 nm) modeled by a Porod term [1]. I_d is the angle independent scattering seen at the highest q values and is controlled by the bonded H content [1]. <D> is the volume-fraction-weighted average diameter of the spheres used to fit the solid lines in Figure 1. Since the size distributions are somewhat skewed as shown in the Figure 1 inset, the most probable size, D_{mp}, is listed in Table 2. If one assumes all the Q_N is due to microvoids and neglects anisotropic scattering revealed by the tilting effects, then the maximum possible void fraction can be calculated [1] as listed in the last column of Table 2.

The tilting data from 1-Al yielded a tilt ratio $Q_N(0^o)/Q_N(45^o) = 1.6$. Since this value is larger than unity, the scattering objects cannot be spherical, but they may be thought of as ellipsoids of revolution, in which case the diameters used in the fitting will be the minor-axis diameters of the ellipsoids. Using the ellipsoidal model [1], a correction to the values of Q_N (0^o) can be made in order to account for the forward scattering of the oriented objects and estimate a correction to the values of the maximum possible void fractions. This correction reduces f_{max} from 0.15 vol.% to 0.11 vol.%. Assuming the other two sample show a similar tilt effect, then the f_{max} values listed in Table 2 will by reduced about 30%. The average major-to-minor axis ratio can also be estimated from the above tilt ratio to be about 2.2 based on the assumed ellipsoidal shapes.

The XRD patterns obtained from the 3 films on the stainless steel are shown in Figure 2. These were run with long scan times to obtain data of good statistical quality. Also shown is the pattern from the back of one of the SS samples. The extra peaks from the 50 nm μc-Si layer of

3-SS are clearly seen. A procedure was used to subtract the SS background from each of the sample patterns [2] and these results are shown in Fig. 3. These patterns were then computer fitted to obtain quantitative values of the full-width-at-half-maximum (FWHM) and position (P) of the first sharp peak (FSP) of the intrinsic a-Si:H layer [2]. Table 3 lists the quantitative results from these fits.

Table 3. Quantitative XRD results. I_T = total integrated intensity of both a-Si:H peaks. Statistical uncertainties in the last significant figures are given in parentheses.

Sample No.	FWHM (2θ-deg)	P (2θ-deg)	I_T (deg-c/s)
1-SS	5.59(9)	27.59(2)	229
2-SS	5.55(9)	27.58(2)	236
3-SS	5.29(11)	27.64(4)	234

The similar values of I_T are consistent with all i-layers having the same thickness of 2 μm. The sample 3-SS was carefully fitted to include the μc-Si:H peaks corresponding to the (111), (220), and (311) peaks at 28.41°, 47.39°, and 55.8°, respectively. The integrated intensities of these peaks amounted to about 3% of I_T, consistent with 50 nm compared to 2000 nm.

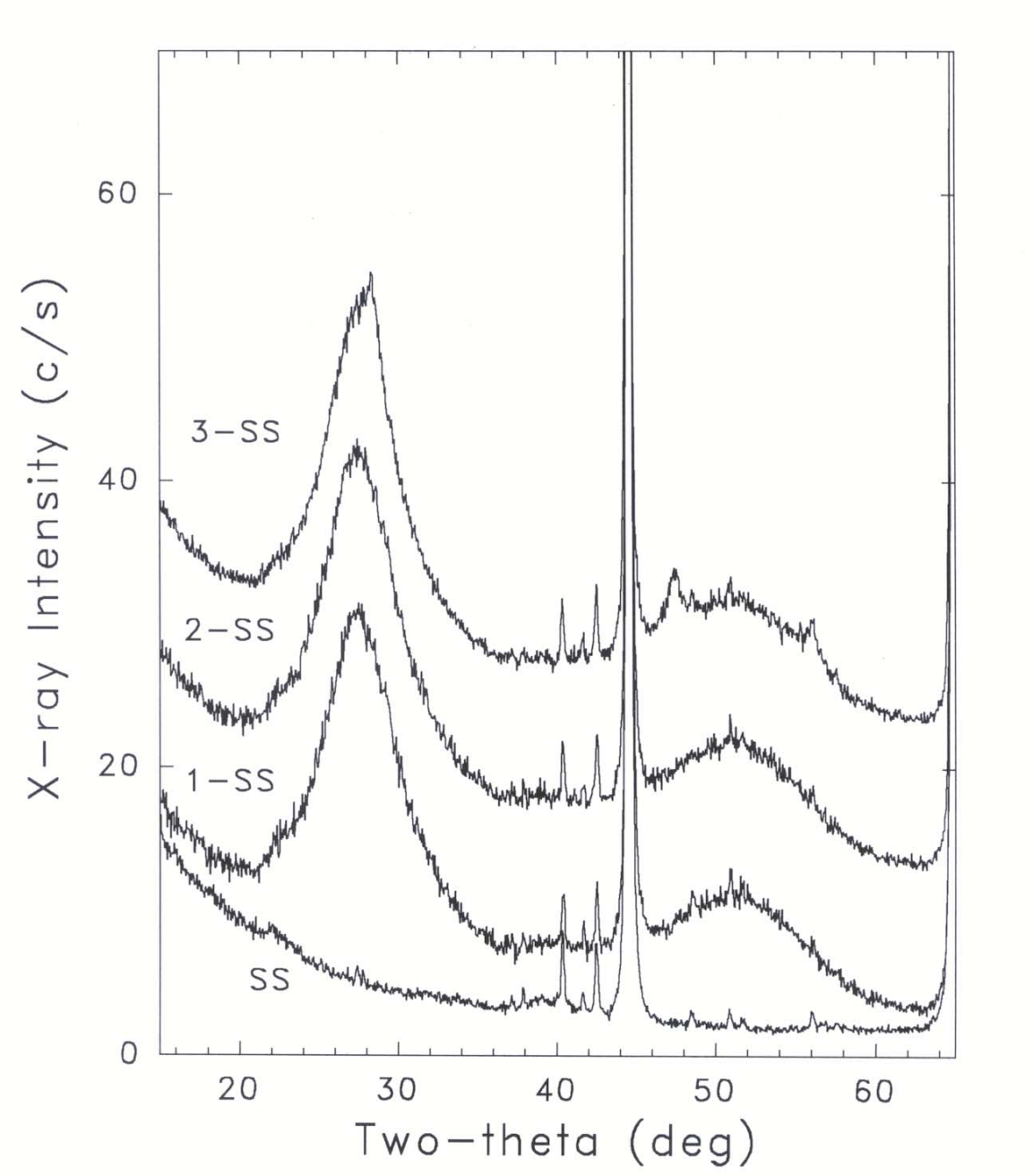

Fig. 2. XRD patterns from the three Utrecht films on stainless steel. Reference pattern from stainless steel only (SS) also shown.

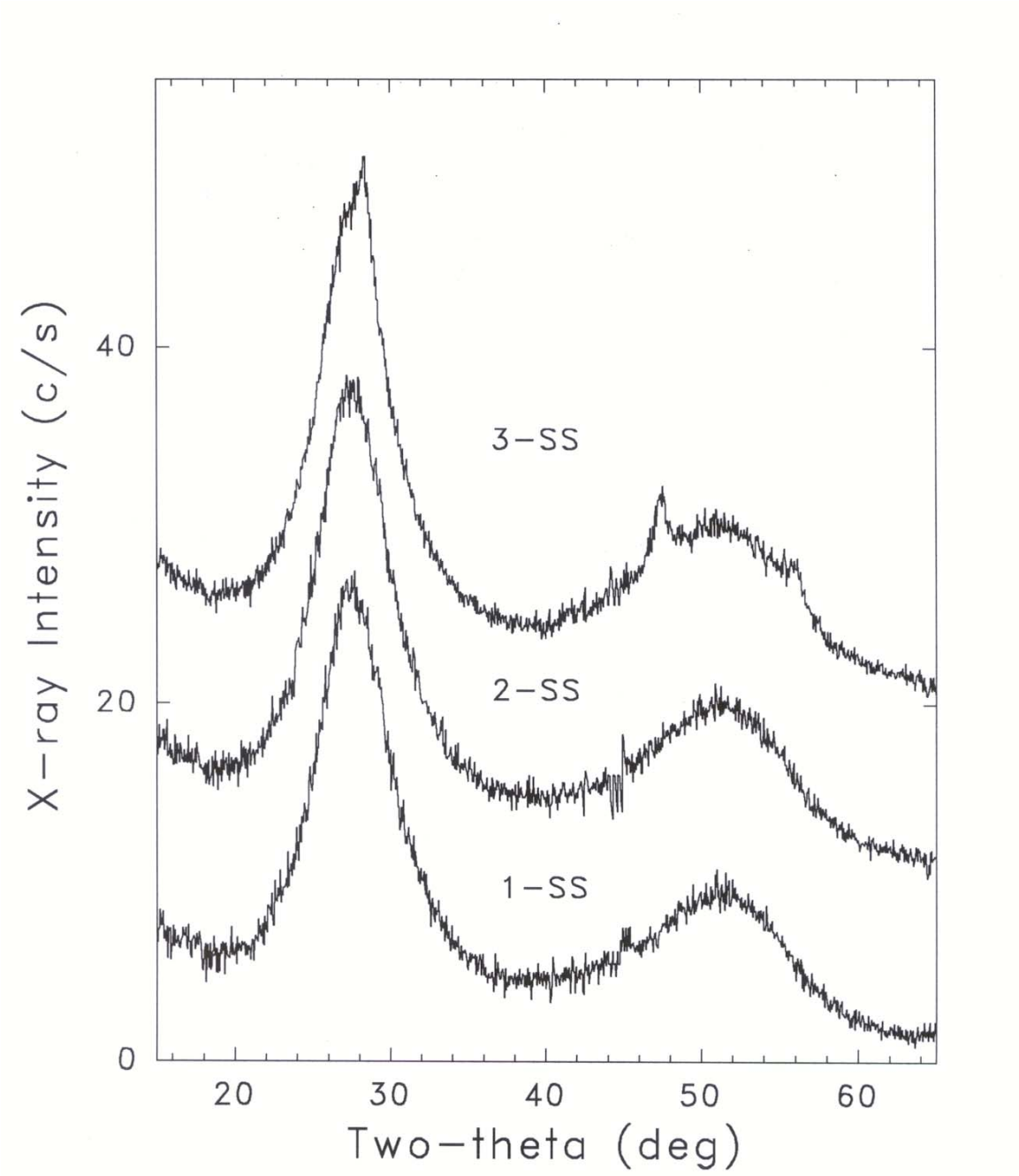

Fig 3. XRD patterns from three Utrecht films after subtraction of SS reference pattern.

The flotation density was measured by the technique summarized in [3]. Pieces of the SAXS films on Al foil were used for these measurements. Results for the 3 films are listed in Table 4. The uncertainty is based on reproducibility in repeated measurements. The H content in the amorphous phase, C_H, can be estimated based on an established correlation [3] between density and C_H in a fully amorphous film: ρ (in g/cm^3) = 2.291-0.0068C_H(in at.%). This yields the C_H values in Table 4. If we also correct for the maximum possible void fractions given in Table 2, then the flotation densities are first adjusted by the f_{max}: $\rho(1+0.01f_{max})$ and then used in the above equation to yield modified C_H values. However, these corrections change C_H by less than 1% due to the small void fractions. The slightly lower C_H for 3-Al seems consistent with a slightly lower I_d (Table 2) which is proportional to C_H [1].

Table 4. Flotation density results.

Sample No.	ρ (g/cm^3)	C_H (at.%)
1-Al	2.194(5)	14
2-Al	2.197(5)	14
3-Al	2.219(5)	11

It would be interesting to compare these results with IR-based H contents from similarly prepared samples.

Summary Comments:

1) The SAXS Q_N and associated void densities are quite similar for all three films. It is quite likely that the extra SAXS signal from 3-Al is due to the 50 nm μc-Si layer since it is well known that SAXS from μc-Si:H is quite strong [3]. It may be that the actual Q_N from only the a-Si:H intrinsic layer of 3-Al is less than in Table 2 and therefore the f_{max} may be less. In any case, for all three films, the void density is quite low but significantly higher than the best device quality PECVD and HWCVD material where Q_N is near the detection limit of about 2x10^{22} eu/cm^3 corresponding to 0.01 vol.% [1].

2) The size distributions of the scattering features based on fitting of spherical (or ellipsoidal) shapes are all quite similar with most probable sizes of only 2 or 3 nm. It would be interesting to compare these results with the TEM results from Utrecht.
3) The XRD results support the earlier results that the intrinsic film grown on the μc-Si(n) template has an improved medium range order based on the narrower FWHM for this film compared to the film grown directly on the SS. However, the film grown on the a-Si(n) template does not seem to be improved.
4) The flotation densities are explained mainly by the effects of bonded H on the density rather than by void fractions since the latter are quite low based on the SAXS.

1. D.L. Williamson, Mat. Res. Soc. Symp. Proc. **377** (1995) 251.
2. D.L. Williamson, Mat. Res. Soc. Symp. Proc. **557** (1999) 251.
3. D.L. Williamson, Solar Energy Mats. and Solar Cells **78** (2003) 41.

Task 3

Several films of a-SiGe:H made by HWCVD were supplied by NREL to examine the XRD features, mainly the widths of the first sharp peak (FSP) in the diffraction patterns. The goal was to search for any differences in medium range order induced by the different filaments Ta and W.

The table below summarizes the XRD results. There is no obvious trend in FWHM. The similar values of integrated intensity indicate similar thicknesses for the films and the slightly lower value for the half-sized L1230 suggests some of the intensity is lost due to too small a sample size. The peak positions are all significantly smaller than a-Si:H, typically around 27.6 degrees, consistent with significant Ge contents and therefore a larger average interatomic distance.

Table of XRD Results from a-SiGe:H Films. Uncertainties in parentheses. I_T is the integrated intensity of the FSP.

Sample	Filament	FSP-FWHM (deg)	I_T (deg-C/S)	P (deg)
L1230	Ta	5.49 (15)	39	27.18 (8)
L1230(half-size)	Ta	5.41 (20)	30	27.28 (8)
L1232	Ta	5.27 (15)	39	27.05 (8)
L898	W	5.18 (20)	32	27.18 (8)
L907	W	5.18 (15)	39	27.27 (8)
L911	W	5.59 (20)	32	27.31 (8)